Infrared chemiluminescence studies of the reactions of H atoms with CCl_3, CF_2Cl, and CH_2CH_2Cl radicals at 300 and 475 K: recombination–elimination vs. abstraction mechanisms

E. ARUNAN,[1] R. RENGARAJAN, AND D.W. SETSER[2]

Department of Chemistry, Kansas State University, Manhattan, KS 66506, U.S.A.

Received June 9, 1993

This paper is dedicated to Professor John C. Polanyi on the occasion of his 65th birthday

E. ARUNAN, R. RENGARAJAN, and D.W. SETSER. Can. J. Chem. **72**, 568 (1994).

The reactions of H atoms with CCl_3, CF_2Cl, and CH_2CH_2Cl radicals have been studied in a flow reactor at 300 and 475 K by observation of the infrared emission from the HCl and HF products. These reactions were observed as secondary reactions from the H + CCl_3Br, CF_2ClBr, and CH_2Cl–CH_2I chemical systems. The conditions in the flow reactor were controlled so that the nascent vibrational distributions of HCl and HF were recorded. The pattern of vibrational energy disposal to HCl was used to differentiate between Cl atom abstraction and recombination–elimination mechanisms. The H atom reactions with CCl_3 and CF_2Cl radicals occur only via a recombination–elimination mechanism and give HCl(v) or HF(v) in a unimolecular step. Thus, the Cl atom abstraction reactions must have $\geq$3.0 kcal mol^{-1} higher activation energy than the recombination reaction. From observation of the ratio of the HCl and HF products from CHF_2Cl^*, the difference in threshold energies for HF and HCl elimination was determined to be ~13 kcal mol^{-1}. On the other hand, Cl atom abstraction does compete with recombination–elimination in the H + CH_2CH_2Cl reaction, the branching fraction is ~0.3 at 300 K and ~0.6 at 475 K.

E. ARUNAN, R. RENGARAJAN et D.W. SETSER. Can. J. Chem. **72**, 568 (1994).

Opérant dans un réacteur à écoulement, à 300 et 475 K, et faisant appel à l'observation de l'émission en infrarouge du HCl et du HF produits, on a étudié les réactions des atomes de H avec les radicaux CCl_3, CF_2Cl et CH_2CH_2Cl. On a observé ces réactions sous la forme de réactions secondaires des systèmes chimiques H + CCl_3Br, CF_2ClBr et CH_2Cl–CH_2I. Les conditions présentes dans le réacteur à écoulement sont contrôlées d'une façon telle que les distributions vibrationnelles naissantes du HCl et du HF puissent être enregistrées. On a utilisé les patrons de distribution de l'énergie vibrationnelle du HCl pour différencier entre les mécanismes d'enlèvement d'atome de Cl et d'élimination–recombinaison. Les réactions des atomes de H avec les radicaux CCl_3 et CF_2Cl ne se produisent que par un mécanisme d'élimination–recombinaison et elles conduisent à du HCl(v) et du HF(v) dans une étape unimoléculaire. Les réactions d'enlèvement d'atome de Cl doivent donc avoir une énergie d'activation qui est $\geq$3,0 kcal mol^{-1} plus élevée que celle de la réaction de recombinaison. En se basant sur le rapport de HCl et HF produits à partir du CHF_2Cl^*, on a déterminé que la différence entre les énergies seuils pour l'élimination de HF et de HCl doit être −13 kcal mol^{-1}. Par ailleurs, l'enlèvement de l'atome de Cl est en compétition avec la réaction de recombinaison–élimination dans la réaction de H + CH_2CH_2Cl; la fraction de bifurcation est d'environ 0,3 à 300 K et d'environ 0,6 à 475 K.

[Traduit par la rédaction]

I. Introduction

The reactions of H atoms with CCl_3, CF_2Cl, and CH_2CH_2Cl radicals at 300 and 475 K have been studied by observation of the HCl and (or) HF product from the infrared chemiluminescence in a fast flow reactor (1–3). The objective was to employ the characteristic vibrational energy disposal patterns to differentiate between the unimolecular HCl or HF elimination reactions from fluorochloromethanes and ethanes (4–7) formed by H-atom recombination vs. the direct, bimolecular Cl-atom abstraction reactions by H atoms (3, 4, 8), even though the two pathways give the same chemical products. The pathway that we identify as Cl-atom abstraction frequently is called a disproportionation reaction in the free radical literature. The current experiments are a logical extension of our earlier report on the room temperature reactions of H with CF_3, CH_2CH_2F, CH_2CF_3, and other fluorine-containing organic radicals (5). These systems exclusively react by the H-atom recombination, HF-elimination pathway because abstraction of F atoms has a high activation energy, and these reactions can serve to define the typical energy disposal pattern for three- and four-centered HF-elimination reactions. Other studies in the literature (6), especially from multiphoton infrared excitation (9) and classical chemical activation (10), show that the dynamics for unimolecular HCl and HF elimination should be similar. The fundamental thesis of the present analysis is that direct abstraction can be identified by examination of the HCl(v) distributions, since the mean fraction of the vibrational energy released to HCl for direct Cl-atom abstraction will be 0.35–0.50 with an inverted distribution (3, 8), whereas the distribution for HCl elimination is expected to be non-inverted with $\langle f_V \rangle \sim 0.15$ (5–7).

The three reaction systems that were studied in the present work are summarized below with the ΔH_0^0 in kcal mol^{-1} given in parentheses. Reactions [1a], [2a], and [3a] represent the recombination plus unimolecular elimination mechanism. Reactions [1b], [2b], and [3b] represent direct abstraction on the singlet or triplet potentials.

$$[1a]\quad H + CCl_3 \rightarrow CHCl_3^* \rightarrow CCl_2(\tilde{X}^1A_1) + HCl \qquad (-41)$$

$$[1b]\quad \rightarrow CCl_2(\tilde{X}^1A_1 \text{ or } \tilde{a}^3B_1) + HCl \qquad (-41 \text{ or } -29)$$

$$[2a]\quad H + CF_2Cl \rightarrow CHF_2Cl^* \rightarrow CF_2(\tilde{X}^1A_1) + HCl \qquad (-54)$$

$$[2b]\quad \rightarrow CF_2(\tilde{X}^1A_1 \text{ or } \tilde{a}^3B_1) + HCl \qquad (-54 \text{ or } 4)$$

$$[2c]\quad \rightarrow CHF_2Cl^* \rightarrow CFCl(\tilde{X}^1A') + HF \qquad (-46)$$

$$[3a]\quad H + CH_2CH_2Cl \rightarrow CH_3CH_2Cl^* \rightarrow HCl + C_2H_4 \qquad (-84)$$

$$[3b]\quad \rightarrow HCl + C_2H_4 \qquad (-84)$$

[1]Present address: Department of Chemistry, University of Illinois at Urbana-Champaign, Urbana, IL 61801, U.S.A.

[2]Author to whom correspondence may be addressed.

TABLE 1. Thermochemistry[a] for the addition–elimination unimolecular reactions

Molecule	$\langle E\rangle^b$	ΔH_0^{0c}	$E_0^{\ddagger d}$	$\langle E\rangle - \Delta H_0^{0e}$	E_p^f	E_x^g
$CH_3CH_2Cl^*(-HCl)$	105.0 ± 2.0	17.0 ± 0.2	55.0 ± 2.0	88.0 ± 2.0	38.0 ± 2.0	50.0 ± 2.0
$CHF_2Cl^*(-HCl)$	102.0 ± 2.0	48.2 ± 2.0	57.0 ± 3.8	53.8 ± 2.0	8.8 ± 3.8	45.0 ± 3.8
$CHF_2Cl^*(-HF)$	102.0 ± 2.0	53.5 ± 4.0	70 ± 4	48.5 ± 4.0	16.5 ± 4.0	32.0 ± 4.0
$CHCl_3^*(-HCl)$	95.5 ± 2.0	55.0 ± 2.0	≈60[h]	40.5 ± 4.0	≈5.0	≈35.0

[a]All entries are in kcal mol^{-1} for reaction on the singlet potential surface.
[b]The total available energy released to the molecule from reactions [1*a*], [2*a*], and [3*a*] for 450 K experiments. The energy for CH_3CH_2Cl is reduced to 103.6 kcal mol^{-1} at 300 K.
[c]The enthalpy change for elimination of HCl (or HF) from the molecule.
[d]The threshold energy for HCl (or HF) elimination; see text for references. The $E_0^{\ddagger}$(HF) for CHF_2Cl was assigned in this work, see text.
[e]Total energy available to the products for the elimination pathway is $\langle E\rangle - \Delta H_0^0$; the available energy for abstraction could be slightly higher if there is an activation energy.
[f]Potential energy released during the reaction, $E_0^{\ddagger} - \Delta H_0^0$.
[g]Excess energy, $\langle E\rangle - E_0^{\ddagger}$, released during the reaction.
[h]The $E_0^{\ddagger}$ from ref. 12 is lower than the currently accepted ΔH_0^0. The reverse reaction is also likely to have a barrier, and $E_0^{\ddagger}$ was set at 60 kcal mol^{-1}.

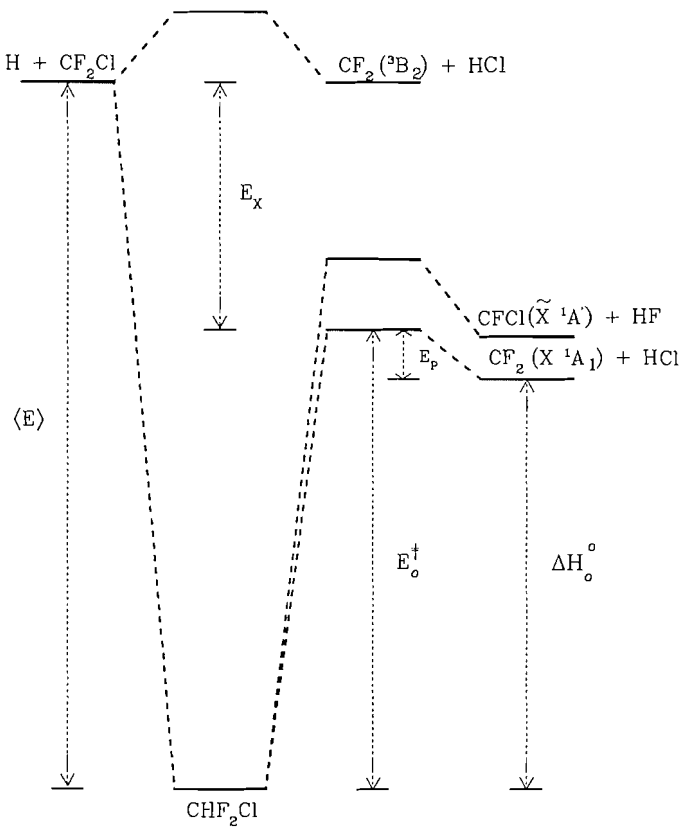

FIG. 1. Schematic representation of the reaction profile for the three-centered elimination reactions of H + CF_2Cl. The diagram is similar for four-centered elimination, but E_p is larger. The values for the energy quantities are given in Table 1.

Direct abstraction of F from CF_2Cl would have a larger activation energy than Cl abstraction, so that reaction is not listed for reaction [2]. The ground states of CCl_2, CF_2, and CFCl are the singlet states; thus, the potential surfaces that correlate to the triplet carbene states lie above the singlet potential surfaces. The recombination–elimination pathways are expected to involve only the singlet potentials. In principle, the Cl-atom abstraction reactions can proceed on either surface, but the singlet potentials probably have lower activation energy.

The HCl channel from CHF_2Cl^* previously was observed (5) using the F + CHFCl reaction to generate CHF_2Cl^*. The HF channel could not be observed in that work because of the strong HF emission from the primary reaction. The thermochemistry for the unimolecular reactions corresponding to [1*a*], [2*a*], and [3*a*] is summarized in Table 1 for 450 K and the symbols are defined in Fig. 1. The average energies of the molecules are given by $\langle E\rangle = D_0(H - R) + E_a(H + R) + nRT$ where E_a is the activation energy and nRT is the thermal energy of the H atom and radical reactants; the energies are $\gtrsim$100 kcal mol^{-1}. The activation energies were taken as zero. The C—H bond energies, D_0, for reactions [1]–[3] were obtained from ref. 11. The threshold energies, $E_0^{\ddagger}$, for HCl elimination from CH_3CH_2Cl (10*a*) and CHF_2Cl (12) were obtained from the literature. The E_a given in ref. 12 for the $CHCl_2$ reaction is smaller than the currently favored ΔH^0 for the reaction, which cannot be true. Also, the reverse reaction, CCl_2 + HCl, is likely to have a small barrier. Allowing for a 5 kcal mol^{-1} barrier for the reverse reaction, $E_0^{\ddagger}$ was set at 60 kcal mol^{-1} for reaction [1*a*]. The $E_0^{\ddagger}$ for HF elimination from CHF_2Cl was assigned from the ratio of rate constants for HF and HCl elimination and $E_0^{\ddagger}$(HCl) (12). The $\Delta H_{f0}^0(CF_2) = -42.6$ kcal mol^{-1} was taken from ref. 13*c* and $\Delta H_{f0}^0(CCl_2) = -52.1$ kcal mol^{-1} was taken from recent experimental work (13*a*, *b*). The thermochemistry for CFCl is not firmly established. We prefer the theoretical estimates of Francisco et al. (14*a*) ($\Delta H_{f0}^0 \approx 7$ kcal mol^{-1}) and Rodriquez and Hopkinson (14*b*) ($\Delta H_{f0}^0 = 3.3$ kcal mol^{-1}) over the experimental estimate of Lias et al. (15) ($\Delta H_{f0}^0 = -2 \pm 7$ kcal mol^{-1}), and we used 5 kcal mol^{-1}. The energy that would be available to the products from abstraction on the singlet surfaces would be larger than the value given in column 5 of Table 1 by the difference in E_a values for abstraction vs. recombination. The least certain values in Table 1 are the threshold energies for the three-centered elimination reactions. This affects the E_p values, which also are the threshold energies for addition of the carbenes to HCl or HF.

Reactions [1]–[3] were observed as secondary steps in a flow reactor containing excess H atoms with the precursor molecules CCl_3Br, CF_2ClBr, CH_2Cl–CH_2I (and also CH_2Cl–CH_2Br), respectively. Previously, we had used only iodine containing precursor molecules for generating the radicals (5). However, the primary reactions with some bromine-containing molecules are sufficiently fast, especially at 475 K, that they can augment the supply of useful precursor molecules for studies of H atom + radical reactions in our flow reactor. The HBr(v) chemilumines-

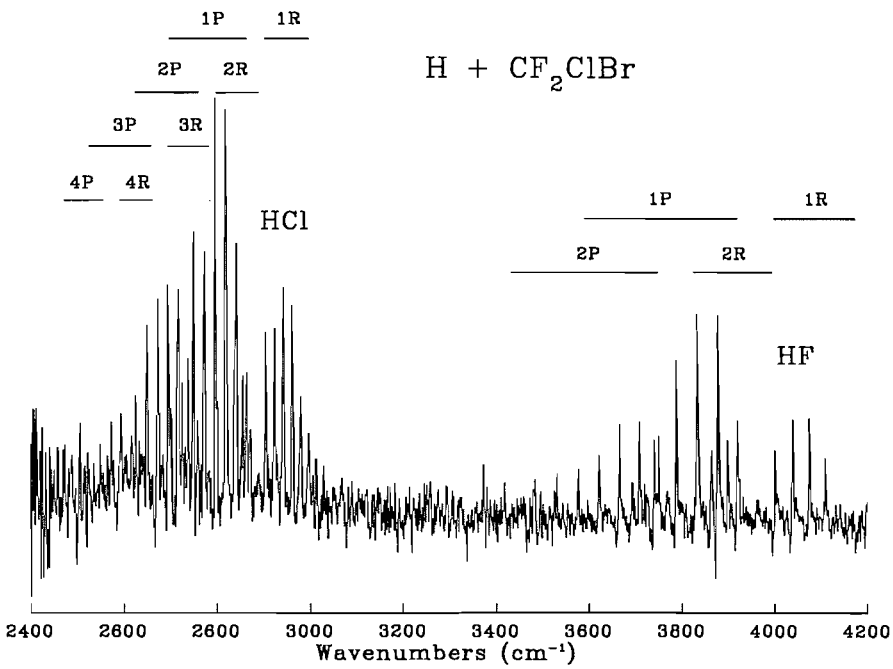

FIG. 2. Infrared emission spectrum from the H + CF_2ClBr system; the concentrations are 3.0×10^{13} and 2.0×10^{13} for [H] and [CF_2ClBr], respectively, and the reaction time is 0.5 ms.

cence from the primary steps could be observed, but the data are not very interesting because only HBr ($v = 0$ and 1) are generated. The H + CF_3 (generated from H + CF_3I) reaction also was studied at 475 K as a reference reaction, and the energy disposal pattern to HF was the same as in our previous room temperature study (5).

The vibrationally excited chloromethane and chloroethane molecules can be collisionally stabilized at high pressure (10), so the abstraction and addition–elimination mechanisms actually become identifiable in terms of the chemical products at high pressure. Dobis and Benson (16) recently emphasized that chlorination of hydrocarbons is an especially effective means to crack hydrocarbons because the recombination steps and direct abstraction (disproportionation) give olefins + HCl. The present work also has relevance to recent work for H + vinyl chloride kinetics (17). Typical values of disproportionation to recombination ratios of alkyl radicals range from 0.1 to 0.5 (18, 19). The question of direct abstraction vs. atom recombination at the radical site followed by unimolecular decomposition is of general importance for the interactions of open-shell atoms and polyatomic radicals. The infrared chemiluminescence technique may be one way to search for these abstraction reactions in atom plus radical encounters.

II. Experimental methods

The experimental method employed the reaction of excess H atoms with precursor molecules in a linear flow reactor. The H atoms were generated by a microwave discharge in H_2–Ar mixtures, and they were introduced at the front of the reactor. Additional Ar carrier gas was added separately at the entrance of the reactor to achieve a total pressure of 0.5–1.0 Torr (1 Torr = 133.3 Pa). The CF_3I, CCl_3Br, CF_2ClBr, and CH_2Cl–CH_2I (or CH_2Cl–CH_2Br) reagents were added via a ring injector 40 cm downstream from the H-atom inlet as a 5–10% mixture in Ar just before the observation window (a 4 cm diameter NaCl flat). Typical concentrations of H and the organic reagent were $(1–3) \times 10^{13}$ and $(0.5–5.0) \times 10^{13}$ molecules cm^{-3}, respectively. The H-atom concentration was assigned from measurement of 50% dissociation of the H_2. For some experiments the CH_2ClCH_2I (or CCl_3Br) was added by flowing Ar over the liquid sample at 300 K. Variable temperature experiments were done by heating the portion of the flow reactor extending from the H_2 and Ar inlets to the observation window (40 cm). The temperature of the reactor was regulated by the voltage supplied to the heating tapes. The temperature of the gas at the downstream edge of the NaCl window was measured with a thermocouple. This temperature was always the same as the temperature of the Boltzmann rotational distribution for HX(v) that was assigned from the emission spectra.

The highest possible flow velocity was ≈ 120 m s^{-1}, corresponding to a reaction time of ~0.2 ms for a reaction zone of 2.5 cm. The Ar pressure could be varied from 0.3 to 1.0 Torr without loss of pumping speed. The HF(v) and HCl(v) vibrational relaxation was fully arrested for these conditions and the rotational relaxation of HF was partly arrested (5, 20). Increasing the reaction time to ≈0.5 ms was required to observe some of the secondary reactions. For these conditions the vibrational distributions from the secondary reaction are hardly affected by relaxation, and the observed distributions are close to the nascent ones. Since HX emission could be observed from H + CF_3 and H + CH_2CH_2Cl (from CH_2ClCH_2I) for the fastest flow speed, we used these reactions for monitoring the degree of vibrational relaxation for other operating conditions.

The emission spectra were recorded at 1–2 cm^{-1} resolution with a Biorad (FTS-60) spectrometer; the individual rotational lines are easily observed, as shown in Fig. 2. A quartz filter with a cutoff at ≈ 2200 cm^{-1} was used to reduce the blackbody radiation for experiments at elevated temperature. The gain on the InSb detector also was reduced to avoid saturation. The rotational population in individual levels was obtained from the peak height of each vibrational–rotational line after division by the instrumental response function and the Einstein coefficient for the particular transition. Improved Einstein coefficients are available for HF and HCl, and their reliability should be better than 5% (21). The HBr coefficients (22) probably are less reliable, but only qualitative observations were made for HBr(v). The HCl and HBr rotational distributions were always Boltzmann at the temperature of the reactor. For some reactions, e.g., H + CF_3, the HF($v = 1$) distribution has a small component for $J \geq 8$ in addition to the Boltzmann component. But this was not the case for the H + CF_2Cl reaction.

Commercial tank grade Ar was purified by passage through molec-

TABLE 2. HX(v) distributions from the halomethane elimination reactions[a]

Reaction	P_0	P_1	P_2	P_3	P_4	λ_V	$\langle f_V \rangle_{HX}$[c]
$H + CF_3 \rightarrow HF(v)$[b]		58.0	30.0	10.0	2.0	-5.1 ± 0.7	0.16
	50.0	29.0	15.0	5.0	1.0		(0.06)
$H + CF_2Cl \rightarrow HCl(v)$		58.0	26.5	10.5	5.0	-3.0 ± 0.6	0.13
	45.2	31.7	14.5	5.8	2.7		(0.08)
$\rightarrow HF(v)$		70	27	3	—	-3.0 ± 0.6	(0.12)
	60.4	27.7	10.7	1.2	—		(0.05)
$F + CHFCl \rightarrow HCl(v)$[d]		51.4	26.5	15.1	7.0	-2.2 ± 0.3	0.12
	43.5	28.9	14.9	8.5	3.9		(0.09)
$H + CCl_3 \rightarrow HCl(v)$		73	22	5	—	-2.7 ± 0.4	0.11
	59.8	29.3	8.8	2.0	—		(0.06)

[a]The P_0 values were assigned from linear vibrational surprisal plots. The vibrational distributions did not change significantly for experiments at 300 and 475 K.
[b]Example of a typical three-centered elimination distribution; the $\langle E \rangle - \Delta H_0^0$ is 52 kcal mol^{-1} and the data are from ref. 5.
[c]The number in parentheses is the mean fraction of vibrational energy for the prior distribution.
[d]Data from ref. 5 at 300 K from the F + CH_2FCl reaction system.

ular sieve traps cooled to liquid N_2 temperature. Tank grade H_2 was used without further purification. All reagents were purified by several freeze–pump–thaw cycles before loading. The CF_3I and CH_2ClCH_2I were purchased from PCR Inc. The CCl_3Br, CF_2ClBr, and CH_2Cl–CH_2Br were obtained from Columbia Organic Chemicals Co.

III. Results

A. General observations

The HBr emissions from the primary reaction with CCl_3Br, CF_2ClBr, and CH_2ClCH_2Br were not analyzed in detail, as our interest was in the atom + radical secondary reactions. The H + CH_2ClCH_2I reaction could be studied with maximum pumping speed (120 m s^{-1}) at 300 K and the observed HCl(v) distribution should be nascent, as judged from other extensive studies in this flow reactor. Even if the pumping speed was reduced by a factor of 2, the HCl(v) distribution was unchanged. If the pumping speed was reduced to ~70 m s^{-1}, HCl emission could be observed from the H + CCl_3Br and CF_2ClBr systems. By analogy to the H + CH_2ClCH_2I reaction, these HCl(v) (and HF(v)) distributions should be nascent. For all three systems the distributions were invariant to changes in [H] and [reagent] for the shortest times that could be used. The HF(v) and HCl(v) emission spectrum from H + CF_2ClBr is shown in Fig. 2. The CH_2ClCH_2Br reaction did not give emission at 300 K unless the pumping speed was greatly reduced. The activation energy for Br abstraction from CH_2ClCH_2Br is evidently higher than for CCl_3Br and CF_2ClBr, presumably because of a higher bond energy. With heating to 475 K, HCl emission could be observed from all four reactions. However, even at 475 K, the HCl emission from CH_2ClCH_2Br was observable only for relatively long reaction times, and the HCl(v) distribution was relaxed compared to the data from the CH_2ClCH_2I system. Table 2 gives a summary of the HX(v) distributions observed for the H + CCl_3Br and CF_2ClBr systems. Table 3 summarizes the experimental results from the H + CH_2ClCH_2I system.

The HCl emission arises only from secondary reaction, since Cl abstraction from the parent compounds has a large activation barrier compared to Br or I atom abstraction. As a test of this thesis, an experiment was done with the H + $CHCl_3$ reaction at 475 K, but no HCl emission was observed for our experimental conditions.

We made no effort to extract information from the temperature dependence of the total emission intensities. For the system with small E_a for the primary step, e.g., CF_3I and CH_2ClCH_2I, the HF and HCl emission intensities actually were slightly smaller at 475 K than at 300 K, because the concentrations and reaction time decrease with temperature, providing that the total pressure is constant and the gas flows delivered to the reactor are constant. The HBr emission intensity from CCl_3Br increased with temperature, but the HCl emission intensity was slightly reduced for the higher temperature. One difficulty with trying to interpret the dependence of the total emission intensity on temperature is that the [H] may not be constant because of the change in the rate of H atom recombination on the wall with temperature. Since the secondary reactions have a second-order dependence on [H], any loss of [H] severely affects the H + radical reaction rate. Direct measurement of the [H], at the observation window, is needed before the temperature dependence of the total emission intensities can be interpreted.

TABLE 3. Summary of HCl(v) distributions for H + CH_2ClCH_2I experiments[a]

No.	$[H_2]$[b]	T (K)	P_1	P_2	P_3	P_4	P_5[c]
1	4.1	300	16.7	27.6	30.3	16.2	9.2
2	6.8	300	15.8	27.2	30.5	17.2	9.2
3	10.0	300	18.3	29.0	28.5	15.8	8.3
4	24.0	300	20.8	29.3	27.7	15.0	7.3
5	24.0	300	19.0	28.2	28.0	17.0	7.7
6	10.9	413	13.9	21.3	28.1	22.5	14.2
7	24.0	475	16.4	23.3	24.8	21.5	13.9
8	24.0	475	15.5	22.7	26.0	22.5	13.2

[a]All experiments were carried out at 0.5 Torr Ar for a reaction time of 0.25 ms.
[b]$[H_2]$ in 10^{12} molecules cm^{-3}; the $[CH_2ClCH_2I]$ was fixed at 2.0×10^{13} molecule cm^{-3}.
[c]P_6 could be estimated as 1/2 P_5. For runs 6–8, trace amounts of $v = 7$ were also observed.

B. H + CCl_3

The HCl distribution from this reaction at 300 K was P_1–P_3 = 74:21:5; the distribution observed at 475 K, 72:23:5, was unchanged. These distributions were recorded for a reaction time of 0.4 ms and they were invariant to change in $[CCl_3Br]$ and $[H_2]$. Since the distribution does not change with temperature, HCl(v) seems to arise only from the recombination–elimination mechanism. The available energy is 40 kcal mol^{-1},

TABLE 4. HCl(v) distributions[a] from the H + CH_2CH_2Cl reaction

Condition	P_0	P_1	P_2	P_3	P_4	P_5	P_6	λ_V	f_V
300 K	—	17.4	27.0	28.0	15.6	8.2	3.8	−11.8 ± 0.8	0.20
(exper.)	20.8	13.8	21.4	22.2	12.3	6.5	3.0		
475 K	—	12.9	19.9	26.2	20.9	13.2	6.9	−14.2 ± 0.3	0.25
(exper.)	12.1	13.4	19.6	23.3	19.3	12.3			
Cl + CH_2CH_2	—	39.0	29.0	22.0	10.0			−10.1 ± 0.3	0.18
(elimin.)[b]	29.9	27.3	20.3	15.4	7.1				(0.04)[c]
H + CH_2CH_2Cl	28.8	24.2	18.6	13.0	8.3	4.7	2.4	[c]	0.155
(elimin.)[c]									(0.04)
H + CH_2CH_2Cl	0	0	17.9	32.1	25.0	14.3	10.7	—	0.33
(abstract.)[d]									

[a]The second line for the first three entries includes the P_0 obtained from the linear surprisal plot; the distribution is then renormalized.
[b]From ref. 26. The available energy is 64 kcal mol^{-1}.
[c]Pure elimination distribution calculated using $\lambda_V = -10.1$ and $\langle E \rangle - \Delta H_0^0 = 88$ kcal mol^{-1}. The elimination distribution is slightly different for the two temperatures due to the change in $\langle E \rangle$, but the difference is not significant. The $\langle f_V \rangle$ for the prior distribution is 0.04.
[d]Abstraction distribution obtained by deconvolution of the experimental distribution from the pure elimination distribution. The distribution from abstraction was forced to be the same for both temperatures.

which could give HCl(v = 5); however, the highest observed level was HCl(v = 3). The P_0 was estimated using a linear surprisal analysis, and the overall distribution after renormalizing is P_0–P_3 = 60:29:9:2. The full statistical model was used to calculate the vibrational prior. The λ_V for this reaction was −2.7 and the $\langle f_V \rangle$ was 0.11. To the best of our knowledge, there are no other theoretical or experimental HCl(v) distributions from the unimolecular decomposition of $CHCl_3$* available for comparison. This HCl(v) distribution is characteristic of three-centered elimination reactions with a small E_p (5, 6).

C. $H + CF_2Cl$

The HCl(v) distribution obtained from this reaction was P_1–P_4 = 57.8:27.4:9.4:5.4 at 300 K and 58.0:25.8:11.1:5.1 at 475 K. As demonstrated in Fig. 2, HF(v) emission also was observed. The HF(v) distribution was P_1–P_3 = 70.5:27.0:2.5 and 70.0:27.0:3.0 at 300 and 475 K, respectively. The HCl(v) and HF(v) distributions did not change with temperature and neither did the ratio of HF(v) to HCl(v). These distributions suggest that the HF and HCl are formed solely by unimolecular elimination from CHF_2Cl*. Linear surprisal plots were used to estimate the P_0 values, and the full distributions are given in Table 2. The HCl(v) distribution from CHF_2Cl* previously observed from the F + CHFCl reaction system is also given in Table 2 for comparison. The small difference in the two HCl distributions is a consequence of the larger $\langle E \rangle$ for F + CHFCl, and the $\langle f_V \rangle$ for the two reactions are almost the same: 0.13 and 0.12. The HF(v) distribution from CHF_2Cl is somewhat less extended than the HF(v) distribution from CHF_3 because the available energy is larger for the latter.

The HF and HCl intensities were corrected for the respective Einstein coefficients and instrumental response function to find the HF($v \geq 1$)/HCl($v \geq 1$) ratio, which was 0.17. Including the P_0 values from the surprisal calculations for HCl and HF distributions increases the ratio to 0.24. The CF_2 + HCl channel was observed to be the more important channel in the IRMPD studies of CHF_2Cl* (9*b*, 23). Martinez and Herron (23*a*) did observe CFCl, but they estimated that the CF_2 + HCl channel accounted for 99% of the reaction. The IRMPD experiments have a much lower $\langle E \rangle$ than the chemical activation experiments, and the HF/HCl ratio would be smaller. Our HF/HCl ratio suggests that the $E_0^{\ddagger}$ for the HF channel is ~13 kcal mol^{-1} higher than that of the HCl channel; this estimate was obtained by comparing the sums of states for the HF and HCl elimination transition states, vide infra.

D. $H + CH_2CH_2Cl$

A summary of the experimental results of various [H_2] and temperatures are given in Table 3. The HCl(v) emission intensity was strong and the results were always consistent. The emission was observed after a reaction time of 0.2 ms, and we believe that the HCl(v) distributions are the nascent vibrational distributions. A special search was necessary for HCl(v = 6) emission, since the HCl(6–5) band falls into the region where CO_2 background absorption occurs. Experiments with extensive flushing of the FTIR spectrometer and long time signal averaging gave a spectrum that could be analyzed and the P_5 to P_6 ratio was 2:1. Trace emission from v = 7 also could be seen. The average HCl(v) distribution observed from this reaction at 300 K was P_1–P_6 = 17:27:28:16:8:4. The available energy of 88 kcal mol^{-1} could give up to HCl(v = 11), and the highest observed HCl(v) level does not extend to the thermochemical limit. The HCl(v) distribution at 475 K was even more highly inverted: HCl(v) P_1–P_6 = 13:20:26:21:13:7. These HCl(v) distributions were highly reproducible at these two temperatures and they were invariant to changes of [H] and [CH_2ClCH_2I]. These slightly inverted distributions are very different from the HF(v) vibrational distributions observed from the HF elimination reactions of CH_3CH_2F and CH_3CF_3 (3).

Leone and co-workers (24) have studied the Cl + CH_3CH_2 reaction, which proceeds by the recombination–elimination mechanism to produce HCl(v). Their HCl(v) distribution, which is shown in Table 4, could be fitted with a linear surprisal plot, and the λ_V (−10.1) is very similar to the slope of the linear surprisal plot for HF elimination (5) from CH_3CH_2F and CH_3CF_3. Scaling a λ_V = −10.1 distribution to the energy for reaction [3] gives a "pure" HCl(v) elimination distribution suitable for comparison to our results. The comparison, see Table 4, clearly indicates that the HCl(v) from the H + CH_2CH_2Cl reaction must be the result of more than just the recombination–elimination reaction. We suggest that the observed HCl(v) distribution from H + CH_2CH_2Cl is the sum of recombination–elimination and abstraction components, with abstraction becoming more pronounced as the temperature is increased. Our

attempt to deconvolute the experimental distribution into the components representing the abstraction and elimination pathways is described in Sect. IV.3.

IV. Discussion

A. *Summary of energy disposal for addition–elimination vs. recombination reactions*

Although the chemical identity of the products is the same from recombination–elimination and from direct abstraction, the vibrational energy disposal patterns to the HCl (or HF) products from the two channels should be much different. The chemically activated halomethane and haloethane molecules with $\sim$100 kcal mol^{-1} of energy have unimolecular lifetimes (statistical limit) that range from picosecond (halomethanes) to nanosecond (haloethanes). The unimolecular elimination reactions yield HX(v) distributions that monotonically decline with increasing f_V and the $\langle f_V(HX)\rangle$ values are typically $\approx$0.15 with vibrational surprisal plots that are linear with slightly negative slopes (5–7). The transition state configurations and the dynamics of the HX elimination reactions are reasonably well understood (25–27). Since the excess energy for $CHCl_3$* and CHF_2Cl* is large, and since the formation steps are not state selective, the mode specific reaction pathways (27) found for photoexcited HFCO are not expected to be important. Stated another way, the relaxation of the energy released primarily in the H—C bond is expected to attain a microcanonical distribution before HX elimination occurs (28). In contrast, the characteristic HX(v) distributions from direct Cl or F abstraction by H atoms over repulsive potentials are sharply inverted and rather narrow with $\langle f_V(HX)\rangle = 0.4$; the vibrational surprisals are not linear and the distributions do not extend to the thermochemical limit (3, 4, 8). The rotational energy disposal from elimination and abstraction reactions are both rather modest (4–6), so the rotational energy disposal pattern is not very useful in distinguishing between the two reaction pathways. The energy disposal for Cl atom abstraction from polyatomic molecules by H atoms is representative of the class of reactions in which the dynamics are limited by kinematic constraints associated with the motion of the light H atom over a repulsive surface (3, 4, 8, 22). This pattern of energy disposal was characterized by Polanyi in a classic series of papers dealing with the reactions of H atoms with the diatomic halogen molecules (29).

Recombination reactions of methyl-type radicals with H atoms generally are considered to have nearly zero activation energies with rate constants of (1–2) $\times$ 10^{-10} cm^3 s^{-1} (30), whereas the abstraction pathways could have small positive activation energies. The halogen–carbon bond energies are large, D(Cl—CCl_2) = 62 kcal mol^{-1} and D(F—CF_2) = 87 kcal mol^{-1}, and Cl- or F-atom abstraction to give singlet carbenes is not expected to compete with recombination. Our method of observation would not be sensitive to direct abstraction on the triplet surface for H + CCl_3 and CF_2Cl giving triplet state carbenes because the available energy is rather low; see reactions [1b] and [2b]. The only case where H-atom abstraction might be expected at modest temperatures is H + CH_2CH_2Cl.

B. *HX elimination reactions from halomethanes*

The energy disposals to HX(v) from $CHCl_3$* and CHF_3*, respectively, are similar; but, the HF(v) distribution from CHF_3* does have a slightly larger negative λ_V and a larger $\langle f_V\rangle$. The HF(v) and HCl(v) distributions from CHF_2Cl* are more similar to the $CHCl_3$* reaction. The larger $\langle f_V(HF)\rangle$ from CHF_3* probably arises from the larger potential energy that is released in the exit channel. In our previous work (5), the energy released to the products from unimolecular processes with statistical lifetimes was treated as the sum of the statistical fraction of the excess energy (6), and the fraction of the potential released to HX, e.g., eq. [4].

$$[4]\quad \langle E_V(HX)\rangle = a\langle E_X\rangle + b\langle E_P\rangle$$

For the halomethanes the a value was $\approx$0.1 and the b value was $\approx$0.35. Using these a and b values with the thermochemistry in Table 1 gives good agreement with the experimental $\langle f_V\rangle$ values for $CHCl_3$* and CHF_2Cl*. For example, the $\langle f_V(HCl)\rangle$ for $CHCl_3$* and CHF_2Cl* are calculated to be 0.13 and 0.14 compared to the observed values of 0.11 and 0.13. The E_p is small for these reactions and the energy release is dominated by the excess energy, which is statistically distributed among the modes at the transition state geometry. As already noted, the mode-specific unimolecular rates (27) found for photoexcitation of HFCO at energies near $E_0^{\ddagger}$ are not expected for the highly energized $CHCl_3$* and CHF_2Cl* molecules.

The recombination rate constants (300 K) for H atoms with methyl-type radicals are large, near the orbiting limits (30), and little or no steric requirement exists. If we assume that a 5% contribution to HCl (high v) from abstraction could have been observed, then the activation energy for abstraction must be 3 kcal mol^{-1} (for similar pre-exponential factors for [1a] vs. [1b]). The H-atom reactions with NF_2 (31a), SF_5 (22), and CF_3O (31b) also proceed by addition–elimination mechanisms; however, these bimolecular rate constants are somewhat smaller than for H + methyl-type radicals. Comparison with the ClO (32a)[3] and NFCl (32b) reactions is worthwhile. The unpaired electron in these radicals is in a delocalized π orbital and the H atom seems to add to more than one site. For this reason and also because of the very short HOCl lifetime and a surface crossing in the exit channel, the energy disposal to HCl + O(^3P) differs from the normal HX elimination pattern.

The branching ratio for HF vs. HCl formation from CHF_2Cl* was 0.24 at $\langle E\rangle$ = 102 kcal mol^{-1}. This ratio is equal to the ratio of RRKM rate constants, which reduces to the ratio of sums of states of the two transition states. We assigned frequencies of 1275(1), 1050(2), 800(1), 670(2), 600(2) and 1160(1), 950(2), 780(3), 500(2) to obtain pre-exponential factors of $\sim 1.5 \times 10^{13}$ per reaction path for the thermal rate constants at 800 K for HCl and HF elimination, respectively. For these transition states a $\Delta E_0^{\ddagger}$ difference of 13 $\pm$ 1 kcal mol^{-1} was required to get a branching ratio of 0.12 for a reaction path degeneracy of 1 for each channel.

C. *H + CH_2CH_2Cl reaction*

The HCl(v) distribution and the $\langle f_V(HCl)\rangle$ from this reaction differ from the typical pattern found from the four-centered elimination reactions of CH_3CH_2Cl*, CH_3CH_2F*, and CH_3CF_3*. The recent work of Leone and co-workers (24) in which CH_3CH_2Cl* was formed by the Cl + CH_3CH_2 recombination reaction represents an important benchmark, because the HCl(v) distribution was as expected from a four-centered HX elimination process. Therefore, we infer that the Cl + CH_3CH_2 reaction proceeds entirely by atom–radical recombination fol-

[3]The broken line shown in Fig. 5 of ref. 32a should be ignored; the surprisal plot is not linear.

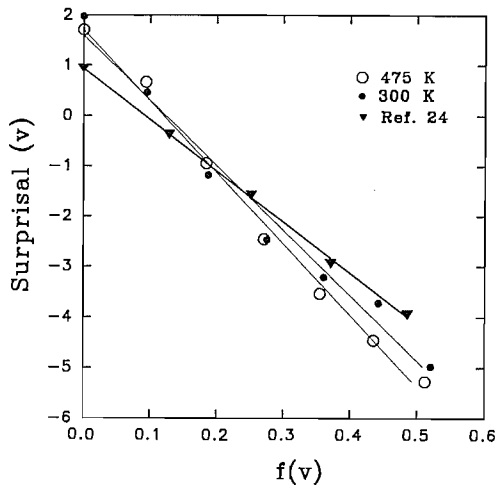

FIG. 3. Surprisal plots for the HCl(v) distributions from H + CH_2CH_2Cl at 300 K (filled circles) and 475 K (open circles) and the Cl + CH_3CH_2 reaction (filled triangles) from ref. 24. Note the smaller slope of the plot from the Cl + CH_3CH_2 reaction.

lowed by subsequent HCl elimination. Since the observed HCl(v) distribution from H + CH_2CH_2Cl differs from the distribution given by Cl + CH_3CH_2, we believe that the former is the sum of a direct abstraction pathway plus a recombination-elimination pathway. Our experiment cannot give the ground state vibrational population, P_0, but some estimate is needed before deconvolution of the experimental distribution can be made into abstraction and elimination components. Since the overall experimental distribution did fit (fortuitously) a linear surprisal plot, extrapolations were used to estimate the experimental P_0 values at both temperatures; see Table 4. The full statistical model for the HCl + CH_2CH_2 products was used to calculate the prior HCl(v) distribution. Figure 3 shows the surprisal plots for our data, and the corresponding plot from the HCl(v) distribution associated with the pure elimination reaction as provided by the Cl + CH_3CH_2 reaction. In some instances, surprisal analysis can distinguish two-component product distributions. However, direct abstraction pathways (by H atoms) do not give linear surprisals, and two linear portions of the surprisal plot for H + CH_2ClCH_2 would not be expected. It is fortuitous, but convenient, that the raw experimental distributions can be represented by a linear surprisal, but with a larger $-\lambda_V$ than for the "pure" elimination distribution.

The CH_3CH_2Cl* formation pathways of H(Cl) + CH_2CH_2-Cl(CH_3CH_2) seem unlikely to be sufficiently state selective to cause nonstatistical unimolecular lifetimes. The main difference in the formation process would be the considerably higher rotational energy carried into CH_3CH_2Cl* by the Cl + CH_3CH_2 recombination reaction. The vibrational energy disposal to HCl from unimolecular reaction of the chemically activated CH_3CH_2Cl* formed by the two recombination reactions should be similar. We used $\lambda_V = -10.1$ with $\langle E \rangle = 105$ kcal mol^{-1} to estimate the "pure" HCl(v) elimination distribution associated with our H + CH_2CH_2Cl reaction. The calculated "pure" HCl(v) distribution is presented in Table 4. There is a very definite difference between this "pure" HCl(v) elimination distribution and our experimental distributions.

Two assumptions are necessary in order to estimate a branching fraction and the HCl(v) distribution for the Cl atom abstraction reaction. We focused attention on the HCl($v = 0$) population

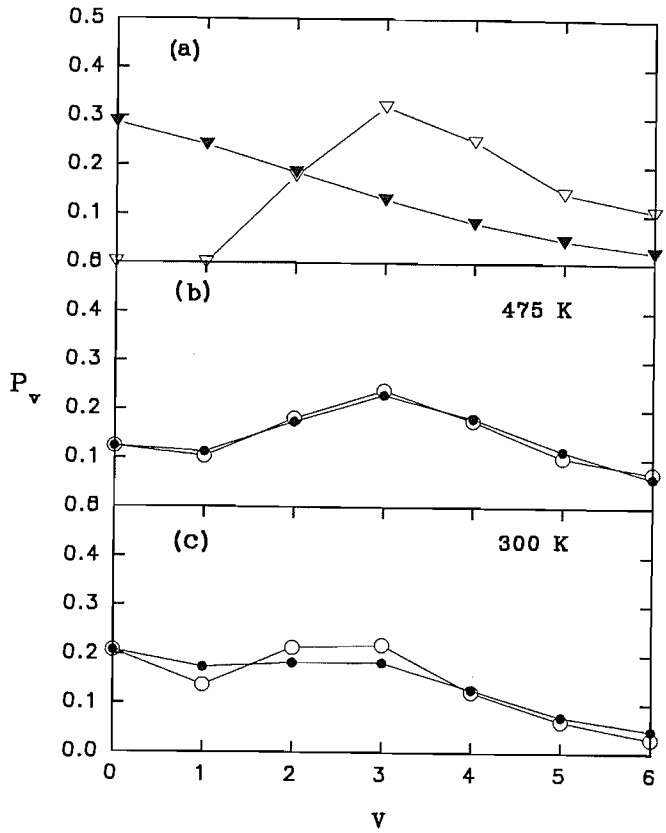

FIG. 4. (*a*) Comparison of the pure elimination (▼) and the abstraction (▽) HCl vibrational distributions from the H + CH_2CH_2Cl reaction. The abstraction distribution is the average distribution that best fits all the experimental distributions. (*b*) The 475 K experimentl distributions are compared to the sum of the two components with weights of 0.57 and 0.43 for abstraction and elimination, respectively. (●)-P_v observed and (○)-P_v calculated. (*c*) Same as Fig. 4*b* except at 300 K with weights of 0.28 and 0.72 for abstraction and elimination, respectively.

and assumed that HCl($v = 0$) arises only from the elimination reaction. This assumption together with using a linear surprisal distribution with $\lambda_V = -10.1$ for the elimination distribution directly leads to the fraction of the reaction going through the abstraction channel, f_a. Thus, f_a was determined to be 0.28 at 300 K and 0.57 at 475 K. To obtain an overall average distribution for abstraction, we assumed that the vibrational distribution from the abstraction channel does not change with temperature and adopted a single distribution for the abstraction process. The deconvolution method is not sufficiently sensitive to extract temperature-dependent distributions for the abstraction reaction. In any event, the change in thermal energy of CH_2ClCH_2 will not affect the HCl(v) distribution for abstraction, which depends on the release of repulsive energy by the potential. The best vibrational distribution for the abstraction channel was selected so that when combined with the "pure" elimination distribution, the experimental distributions were reproduced. Figure 4 shows the two separate components, and the synthetic overall distributions are compared with the experimental ones at 300 and 475 K. The agreement between the synthetic distribution and the experimental ones is satisfactory. The vibrational distribution that was assigned to the abstraction channel is given in the last line of Table 4. The $\langle f_V \rangle$ for this inverted distribution is 0.33, which is similar to the majority of other Cl-atom abstraction reactions from polyatomic inorganic

molecules such as Cl_2O, NO_2Cl, and $NFCl_2$ (32*b*). The derived distribution for the abstraction reaction has a negligible P_1 value. Although the true value may not be zero, a small P_1 is consistent with direct abstraction.

The structure of the chloroethyl radical must closely resemble that for ethyl radical with sp^2 bonding at the localized radical center. The $D_0(Cl—CH_2CH_2)$ is only ~18.5 kcal mol^{-1}, which is lower than for the other Cl-containing polyatomic molecules, such as NO_2Cl, Cl_2O, and $NFCl_2$, that have been studied to obtain HCl(v) distribution. These inorganic molecules have rate constants (3, 31) in the 2×10^{-11} cm^3 molecule^{-1} s^{-1} range at 300 K. Assuming an enhancement in the abstraction rate constant with reduced bond energy, a competition between Cl-atom abstraction and recombination for CH_2CH_2Cl is reasonable. Based on the present knowledge, an abstraction channel from a radical may be expected for radicals with especially weak bond energies at a β-position to the radical center and for radicals with delocalized orbitals containing the unpaired electron (32). The question of abstraction vs. recombination for F + SiH_n (n = 1–3) reactions has been discussed (33). Abstraction seemed to be favored for SiH_2, but the singlet recombination pathways were favored over the triplet abstraction pathways for SiH_3 and SiH.

V. Conclusions

The H + CCl_3 and H + CF_2Cl reactions proceed by recombination, giving $CHCl_3$* and CHF_2Cl* molecules, which subsequently eliminate HCl (or HF) to give monotonically declining HCl(v) vibrational distributions with $\langle f_V \rangle$ equal to ~0.12. The H + CF_2Cl reaction also gives HF(v) + CFCl, and the HF/HCl ratio was assigned as 0.24. This ratio was combined with RRKM calculations and the experimental $E_0^{\ddagger}$(HCl) to estimate $E_0^{\ddagger}$(HF) as 70 kcal mol^{-1}. The small ratio of the HF to HCl strongly suggests that $\Delta H_f^0(HCl) + \Delta H_f^0(CF_2) < \Delta H_f^0(HF) + \Delta H_f^0(CFCl)$. Based upon comparison to the vibrational energy disposal to HCl from the Cl + CH_3CH_2 reaction, both direct Cl abstraction and recombination–elimination reaction pathways were assigned to the H + CH_2CH_2Cl reaction. Separating the two reaction pathways, based on an assumed "pure" HCl(v) elimination distribution, suggests that the branching fraction for abstraction is ~0.3 at 300 K. A weak temperature dependence enhances the abstraction pathway at higher temperature.

Acknowledgments

This work was supported by the National Science Foundation under grant CHE-9120489. We are extremely grateful for permission from Dr. Leone to use the data from ref. 24 prior to publication. We are pleased to contribute this paper in honor of the 65th birthday of Professor Polanyi. The development of the infrared chemiluminescence laboratory at Kansas State University was stimulated by the remarkably successful work of Professor Polanyi in this field.

1. B.S. Agrawalla and D.W. Setser. J. Phys. Chem. **90**, 2450 (1986).
2. S. Wategaonkar and D.W. Setser. J. Chem. Phys. **86**, 4477 (1987).
3. S.J. Wategaonkar and D.W. Setser. J. Chem. Phys. **90**, 251 (1989).
4. (*a*) B.E. Holmes and D.W. Setser. *In* Physical chemistry of fast reactions. Vol. 2. *Edited by* I.W.M. Smith. Planum, New York. 1980; (*b*) B.S. Agrawalla and D.W. Setser. *In* Gas phase chemiluminescence and chemi-ionization. *Edited by* A. Fontijn. Elsevier, Amsterdam. 1985.
5. E. Arunan, S.J. Wategaonkar, and D.W. Setser. J. Phys. Chem. **95**, 1539 (1991).
6. E. Zamir and R.D. Levine. Chem. Phys. **52**, 253 (1980).
7. J.J. Sloan. J. Phys. Chem. **92**, 18 (1988).
8. M.A. Wickramaaratchi, D.W. Setser, B. Hildebrandt, B. Korbitzer, and H. Heydtmann. Chem. Phys. **84**, 105 (1984).
9. (*a*) C.R. Quick, Jr., and C. Wittig. J. Chem. Phys. **72**, 1694 (1980); (*b*) A.S. Sudbo, P.A. Schultz, Y.R. Shen, and Y.T. Lee. J. Chem. Phys. **69**, 2312 (1978).
10. (*a*) K. Dees and D.W. Setser. J. Chem. Phys. **49**, 1193 (1968); (*b*) D.W. Setser, T-S. Lee, and W.C. Danen. J. Phys. Chem. **89**, 5799 (1988); (*c*) D.J. Rakestraw and B.E. Holmes. J. Phys. Chem. **95**, 3968 (1991).
11. (*a*) D.E. McMillen and D.M. Golden. Annu. Rev. Phys. Chem. **33**, 493 (1982); (*b*) K. Miyokawa and E. Tschuikow-Roux. J. Phys. Chem. **96**, 7328 (1992); (*c*) Y. Chen and E. Tschuikow-Roux. J. Phys. Chem. **96**, 7266 (1992).
12. K.P. Schug, H.Gg. Wagner and F. Zabel. Ber. Bunsen-ges. Phys. Chem. **83**, 167 (1979).
13. (*a*) J.A. Paulino and R.R. Squires. J. Am. Chem. Soc. **113**, 5573 (1991); (*b*) D.W. Kohn, E.S.J. Robles, C.F. Logan, and P. Chen. J. Phys. Chem. **97**, 4936 (1993); (*c*) M.W. Chase, Jr., C.A. Davies, J.R. Downey, Jr., D.J. Frurip, R.A. McDonald, and A.N. Syverud. J. Phys. Chem. Ref. Data, **14**, Suppl. No. 1 (1985).
14. (*a*) J.S. Francisco, A.N. Goldstein, Z. Li, Y. Zhao, and I.H. Williams. J. Phys. Chem. **94**, 4791 (1990); (*b*) C.F. Rodriquez and A.C. Hopkinson. J. Phys. Chem. **97**, 849 (1993).
15. S.G. Lias, Z. Karpas and J.F. Liebman. J. Am. Chem. Soc. **107**, 6089 (1985).
16. (*a*) O. Dobis and S.W. Benson. J. Am. Chem. Soc. **112**, 1023 (1990); (*b*) J. Am. Chem. Soc. **113**, 6377 (1991).
17. R.B. Barat and J.W. Bozzelli. J. Phys.Chem. **96**, 2454 (1992).
18. M.J. Lexon, R.M. Marshall, and H. Purnell. J. Chem. Soc. Faraday Trans. **88**, 663 (1992).
19. G.O. Pritchard, S.H. Abbas, J.M. Kennedy, S.J. Paquette, D.B. Hudson, M.A. Meleason, and D.D. Shoemaker. Int. J. Chem. Kinet. **22**, 1051 (1990).
20. E. Arunan, D. Raybone, and D.W. Setser. J. Chem. Phys. **97**, 6348 (1992).
21. E. Arunan, D.W. Setser, and J.F. Ogilvie. J. Chem. Phys. **97**, 1734 (1992).
22. R.J. Malins and D.W. Setser. J. Chem. Phys. **73**, 5666 (1980).
23. (*a*) R.I. Martinez and J.T. Herron. Chem. Phys. Lett. **84**, 180 (1981); (*b*) J.C. Stephenson and D.S. King. J. Chem. Phys. **78**, 1867 (1983).
24. P.W. Seakins, E.L. Woodbridge, and S.R. Leone. J. Phys. Chem. **97**, 5633 (1993).
25. (*a*) S. Kato and K. Morokuma. J. Chem. Phys. **73**, 3900 (1980); (*b*) R.M. Benito and J. Santamaria. J. Phys. Chem. **92**, 5028 (1988); (*c*) L.M. Raff and R.W. Graham. J. Phys. Chem. **92**, 5111 (1988).
26. (*a*) J.D. Goddard and H.F. Schaefer III. J. Chem. Phys. **93**, 4907 (1990); (*b*) J.S. Francisco and Y. Zhao. J. Chem. Phys. **96**, 7586 (1992).
27. (*a*) Y.S. Choi and C.B. Moore. J. Chem. Phys. **97**, 1010 (1992); (*b*) W.H. Green, Jr., C.B. Moore, and W.F. Polik. Annu. Rev. Phys. Chem. **43**, 591 (1992).
28. (*a*) A.B. Trenwith, and B.S. Rabinovitch. J. Phys. Chem. **86**, 3447 (1982); (*b*) W.L. Hase. J. Phys. Chem. **90**, 365 (1986); (*c*) C.R. Park, and J.R. Wiesenfeld. J. Chem. Phys. **95**, 8160 (1991).
29. (*a*) J.C. Polanyi, J.F. Sloan, and J. Wanner. J. Chem. Phys. **13**, 1 (1976); (*b*) J.C. Polanyi, J.L. Schreiber, and J. Sloan. J. Chem. Phys. **9**, 403 (1975); (*c*) K.G. Anlauf, D.S. Horne, R.G. Macdonald, J.C. Polanyi, and K.B. Woodall. J. Chem. Phys. **57**, 1561 (1972); (*d*) J.C. Polanyi. Acc. Chem. Res. **5**, 161(1972).
30. (*a*) R.J. Duchovic and W.L. Hase. J. Chem. Phys. **82**, 3599 (1988); (*b*) K.P. Lim, and J.V. Michael. J. Chem. Phys. **98**, 3919 (1993); (*c*) K.J. Hughes, A.R. Pereira, and M.J. Pilling. Ber. Bunsenges. Phys. Chem. **96**, 1352 (1993).
31. (*a*) R.J. Malins and D.W. Setser. J. Phys. Chem. **85**, 1342 (1981); (*b*) R. Rengarajan and D.W. Setser. J. Phys. Chem. Submitted (1994).

32. (*a*) S.J. Wategaonkar and D.W. Setser. J. Chem. Phys. **90**, 6223 (1989); (*b*) E. Arunan, C.P. Liu, D.W. Setser, J.V. Gilbert, and A.D. Coombe. J. Phys. Chem. In press.

33. K. Sato, H. Yamada, and S. Iwabuchi. J. Chem. Phys. **98**, 2844 (1993).